Enhanced liposomal drug delivery via membrane fusion triggered by dimeric coiled-coil peptides

Zeng, Y.; Shen, M.; Singhal, A.; Sevink, G.J.A.; Crone, N.S.A.; Boyle, A.L.; Kros, A.

RESEARCH ARTICLE

Editor's Choice

NANO · MICRO small

www.small-journal.com

Enhanced Liposomal Drug Delivery Via Membrane Fusion Triggered by Dimeric Coiled-Coil Peptides

Ye Zeng, Mengjie Shen, Ankush Singhal, Geert Jan Agur Sevink, Niek Crone, Aimee L. Boyle, and Alexander Kros**

An ideal nanomedicine system improves the therapeutic efficacy of drugs. However, most nanomedicines enter cells via endosomal/lysosomal pathways and only a small fraction of the cargo enters the cytosol inducing therapeutic effects. To circumvent this inefficiency, alternative approaches are desired. Inspired by fusion machinery found in nature, synthetic lipidated peptide pair E4/K4 is used to induce membrane fusion previously. Peptide K4 interacts specifically with E4, and it has a lipid membrane affinity and resulting in membrane remodeling. To design efficient fusogens with multiple interactions, dimeric K4 variants are synthesized to improve fusion with E4-modified liposomes and cells. The secondary structure and self-assembly of dimers are studied; the parallel PK4 dimer forms temperature-dependent higher-order assemblies, while linear K4 dimers form tetramer-like homodimers. The structures and membrane interactions of PK4 are supported by molecular dynamics simulations. Upon addition of E4, PK4 induced the strongest coiled-coil interaction resulting in a higher liposomal delivery compared to linear dimers and monomer. Using a wide spectrum of endocytosis inhibitors, membrane fusion is found to be the main cellular uptake pathway. Doxorubicin delivery results in efficient cellular uptake and concomitant antitumor efficacy. These findings aid the development of efficient delivery systems of drugs into cells using liposome-cell fusion strategies.

1. Introduction

Nanomedicines have improved drug delivery efficiency by amplifying drug bioavailability, improving pharmacokinetic/pharmacodynamic profiles, and/or minimizing undesired off-target or other side effects of encapsulated drugs.[1] Several nanomedicines based on liposomes, albumin nanoparticle (NP)s, and polymeric micelles have been approved for cancer treatment and other nanomedicine candidates for chemotherapy, hyperthermia, radiation therapy, gene therapy, and immunotherapy are in clinical trials.[2] Nanomedicines have been customized to enter cells through different endocytosis pathways, delivering their cargo to the cell primarily via endosomal/lysosomal escape pathways.[3] However, endocytosis often impedes efficient drug delivery since the majority of the nanomedicine cargo faces endo/lysosomal degradation, lowering the therapeutic efficacy. Therefore, novel drug delivery systems circumventing endo/lysosome pathways and/or entrapment would greatly enhance intracellular drug delivery efficiency.

Peptides have attracted great attention in the nanomedicine field due to their diversity and ease of modification and conjugation to nanoparticles.[4] For example, cell-penetrating peptides (CPPs) have been widely investigated for their cell-penetrating abilities,[5] and chemically synthesized CPPs covalently or noncovalently conjugated to biomaterials greatly enhanced cell penetration and drug efficacy.[6] Besides direct penetration, CPP-cargo conjugates still mainly gain their entry to cells through energy-dependent endocytosis pathways, such as macropinocytosis or clathrin-mediated endocytosis.[7] Moreover, CPP dimerization significantly lowered the peptide concentration required by the Tat–TAR interaction which inhibits human immunodeficiency viruses (HIV)-1,[5a] and elicits potent antitumor effects.[8] Based on the advances made in this field, various CPP-derived peptide therapeutics have been clinically evaluated.[9] Unfortunately, to date there are no CPP-based drug conjugates/nanomedicines approved by the Food and Drug Administration (FDA). This might be due to their lack of cell and tissue specificity, drug delivery inefficiency, slow drug release profile, poor stability, rapid renal clearance, or adverse effects including toxicity.[9b,10] Thus, there is still a pressing need to find alternatives to deliver drugs efficiently into cells.

Membrane fusion is a vital process for the transport of (bio)chemicals across membranes in eukaryotic cells, from the exquisite compartmental organization of cells to the precise

Y. Zeng, M. Shen, A. Singhal, G. J. A. Sevink, N. Crone, A. L. Boyle, A. Kros
Dept. Supramolecular & Biomaterials Chemistry
Leiden Institute of Chemistry
Leiden University
Einsteinweg 55, Leiden 2333 CC, The Netherlands
E-mail: a.l.boyle@chem.leidenuniv.nl; a.kros@chem.leidenuniv.nl

The ORCID identification number(s) for the author(s) of this article can be found under https://doi.org/10.1002/smll.202301133

DOI: 10.1002/smll.202301133

timing of chemical synaptic transmission of nervous system activities.[11] The docking of transport vesicles to the target plasma membrane in neuronal exocytosis is triggered by coiled-coil formation of complementary soluble N-ethylmaleimide-sensitive factor attachment protein receptors (SNARE) protein subunits.[11b] For full fusion to occur, the opposing membranes are brought into close proximity, followed by membrane deformation resulting in lipid exchange and ultimately content mixing.[12] Our rationale to design efficient fusogens is therefore that the ideal fusogen is able to specifically recognize its binding partner and able to interact with lipid membranes in order to induce membrane deformation resulting in lipid exchange and ultimately content exchange without significant leakage. Inspired by the SNARE protein complex, we previously developed complementary K/E coiled-coil peptides conjugated to lipids, which were able to trigger membrane fusion, and induce fast and efficient liposomal drug delivery in vitro and in vivo.[13] Peptide K is an amphipathic helical peptide and was specifically designed to interact with peptide E, but when confined to a membrane, it also interacts with lipid bilayers.[14]

Due to the dual affinity of peptide K to both peptide E and lipid membranes, we herein investigate whether the dimerization of peptide K could enhance liposomal drug delivery to cells. The influence of peptide dimerization on solution properties was studied, in addition to the ability to induce fusion of liposomes with cells to facilitate drug delivery (**Scheme 1**). By varying the position of peptide conjugation, three novel dimer designs were synthesized. Peptide folding, self-assembly, thermal stability, and coiled-coil formation of dimers were studied by circular dichroism (CD) spectroscopy. Homodimer formation of linear K4 dimers and particle formation of parallel K4 dimers was evaluated by employing a CD titration assay and utilizing dynamic light scattering (DLS). Next, we determined the affinity of various K4 dimers for lipid membranes using a tryptophan fluorescence assay, and we evaluated the ability of different coiled-coil pairs to induce membrane fusion by performing lipid-and content-mixing assays. Cell-membrane binding affinities of dimers and cellular uptake of liposomes were evaluated by flow cytometry and confocal microscopy. The in vitro antitumor effect of the chemotherapeutic doxorubicin (DOX) encapsulated in liposomes was quantified as a function of dimer design. These findings not only offer important mechanistic insights into the design of coiled-coil driven membrane fusion systems but also provide novel strategies for developing peptide-based biomaterials.

2. Results and Discussion

2.1. Peptide Design

Peptide Kn (KIAALKE)n was previously designed to form a parallel heterodimeric coiled-coil complex with peptide En (EIAALEK)n,[14a,15] but we discovered it also has a high affinity for fluid phospholipid membranes. Upon membrane binding, peptide K induces positive membrane curvature and destabilization, facilitating membrane fusion.[14b–d] Due to these competing interactions, we rationalized that a peptide K-dimer might interact simultaneously with peptide E as well as with a membrane, resulting in enhanced fusion. How these dual interactions will result in membrane fusion is most likely dependent on the exact structure of these dimers. In this study, we designed three K4-dimers by incorporation of a cysteine, permitting disulfide bond formation. The cysteine was introduced at either the N- or C-terminus, or the f-position of the second heptad of peptide K. Upon cysteine oxidation, the parallel dimer PK4 and the linear dimers NK4 (N-terminal conjugation) and CK4 (C-terminal conjugation) were obtained (Scheme 1a; and Scheme S1, Supporting Information). Based on their structures, we hypothesized linear K4-dimers may form a "tetramer-like" homodimer structure or a hairpin structure in the absence of peptide E. Conversely, as the hydrophobic faces of both K peptides are oriented in opposite directions in PK4, it was expected that this dimer may aggregate and form particles.

2.2. Secondary Structure, and Coiled-Coil Formation of K4 Dimers

The secondary structure of the peptide dimers, and their ability to interact with peptide E, was studied using circular dichroism (CD) spectroscopy. In line with previous studies, monomeric peptide K4 folds into an α-helix as evidenced by the two minima at 208 and 222 nm. Peptides NK4 and CK4 also adopt a highly helical structure; their helicity was higher than the K4 monomer (**Figure 1**a; and Table S3, Supporting Information). In contrast, PK4 adopted a non-α-helical spectrum, indicative of a different secondary structure or self-assembly (Figure 1a; and Table S3, Supporting Information). It is possible that the spectrum obtained with PK4 is a result of light scattering due to aggregation (vide infra).[16]

Next, the interaction of the K4 dimers with peptide E4 was investigated. Peptide E4 adopts an α-helical secondary structure and upon mixing with an equimolar amount of PK4, coiled-coil formation was observed (Figure 1b). The linear dimer NK4 was also shown to interact with E4 (Figure 1c; and Table S3, Supporting Information), however, the CD spectrum of CK4 and E4 did not indicate effective coiled-coil formation (Figure 1d; and Table S3, Supporting Information). This finding suggests that the 'tetramer-like' homodimer or helical hairpin of CK4 is very stable, preventing interaction with E4, but the less stable homodimer of NK4 does form heteromeric coiled coils with E4, as does PK4.

Temperature-dependent CD spectroscopy was applied to determine the thermostability of the peptides (Figure S1a, Supporting Information). Peptide K4 shows a typical sigmoidal melting curve, and the melting temperature (T_m) was determined to be 50 °C. In contrast, the linear K4 dimers NK4 and CK4 remained highly helical over the entire temperature range. Even at 95 °C, a decrease in ellipticity of only 44% and 46%, respectively, was observed, revealing the very high thermal stability of these two K4 dimers. PK4 formed a non-α-helical secondary structure (Figure 1a), and the temperature-dependent CD measurement was also unusual, showing a "V" shaped melting curve with the highest ellipticity at ≈60 °C. To better understand this unusual behavior, full CD spectra of PK4 were measured at different temperatures (Figure S1b, Supporting Information). A signature α-helical CD signal was gradually obtained when the temperature was raised from 5 to 60 °C. Upon further heating to 90 °C, the helical secondary structure disappeared. Thus, PK4 changes from a distorted non-α-helical state to an α-helix, and then eventually to

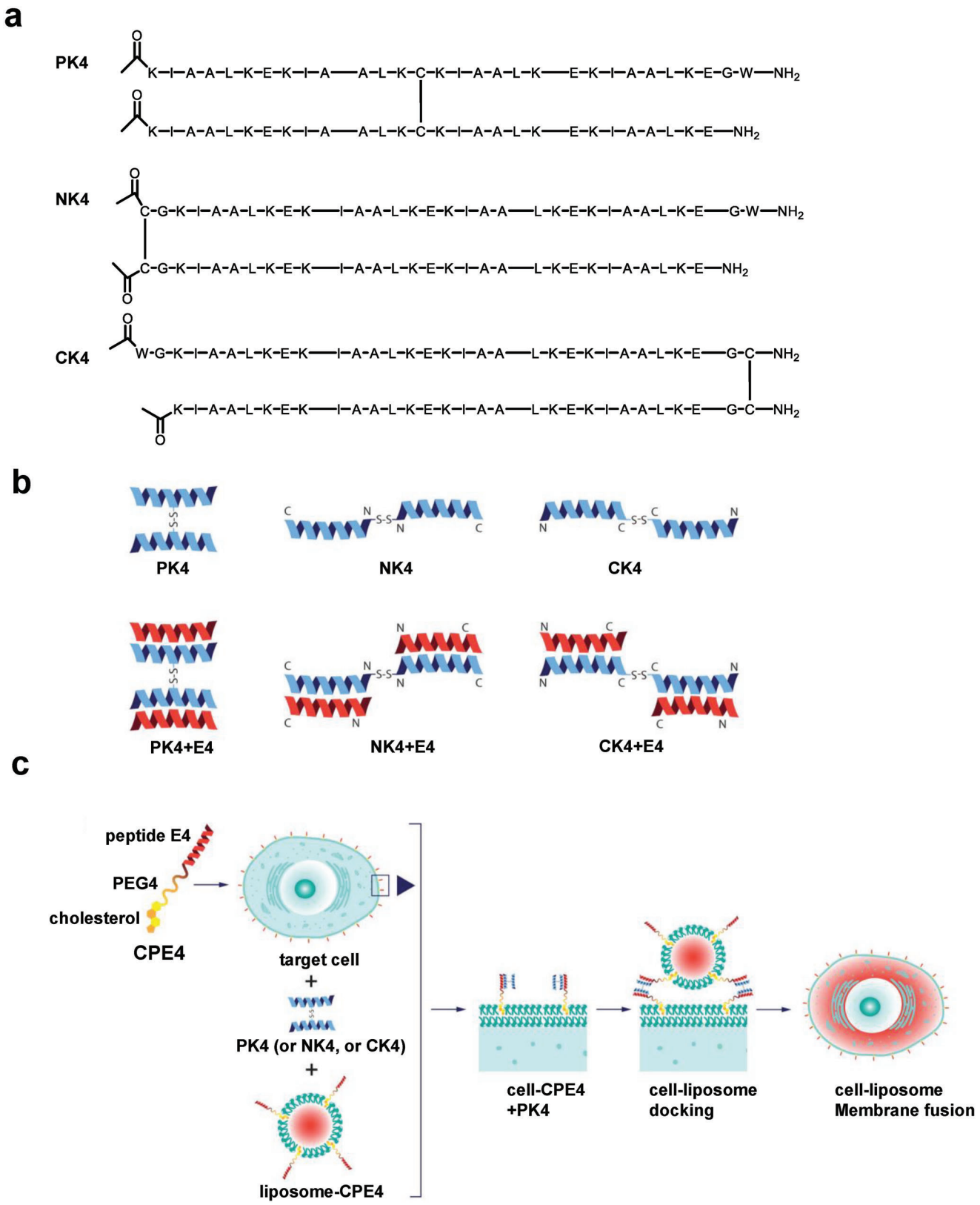

Scheme 1. Schematic illustration of the cell-liposome membrane fusion process trigged by K4-dimers and E4. a) Peptide sequence information of K4 dimers. b) Schematic representation of K4-dimers and coiled-coil structures of K4-dimers with complementary E4 peptides. c) Liposomal drug delivery to cells through membrane fusion induced by different coiled-coil peptides.

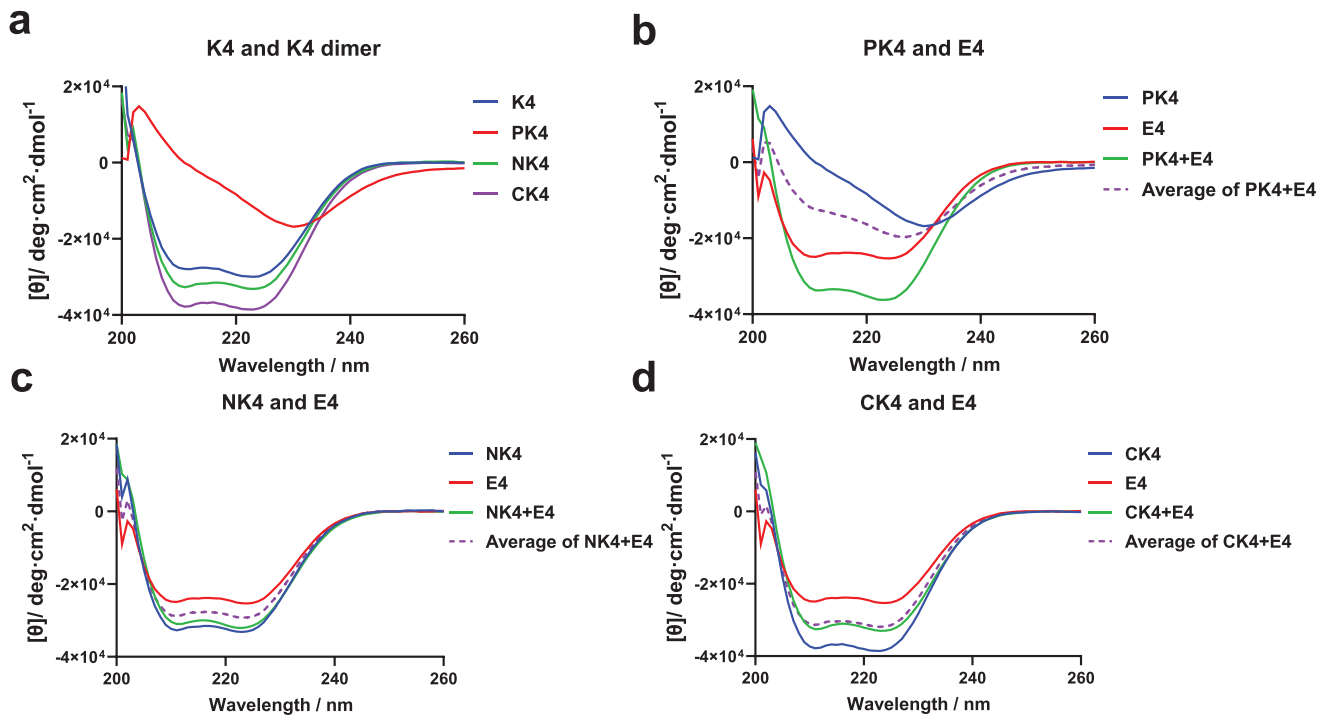

Figure 1. CD spectra of a) K4 monomer and K4-dimers, b) PK4 ± E4, c) NK4 ± E4, and d) CK4 ± E4. Solid lines are measured spectra, dotted lines are calculated average spectra from the K4-dimers and peptide E4. Spectra were recorded in PBS (pH 7.2) at 20 °C. K4-dimer, 5 μM; K4 monomer, 10 μM; E4, 10 μM.

a different nonhelical state, revealing an intriguing temperature-dependent nature of PK4 assembly.

Next, the thermal stability of the helical peptides was determined in the presence of peptide E4 (Figure S1c, Supporting Information). The high thermal stability of NK4 and CK4 was further enhanced in the presence of E4, with only a 30% and 32% decrease in ellipticity upon heating to 90 °C. This suggests that both linear dimers did indeed interact with E4, at least at elevated temperatures. It is also possible that the homodimeric NK4 and CK4 species gradually dissociate to form monomeric species and thus form more stable heterodimers with E4 when the temperature is increased. In contrast, coiled-coils formed by mixing PK4 and E4 show poor thermal stability as an 89% ellipticity decline was observed. Indeed, a typical sigmoidal melting curve was obtained with a T_m of 55 °C. Overall, it can be concluded that the linear K4 dimers have high thermostabilities, which increase further upon the addition of E4. In contrast, PK4 shows complex (self)-assembly behavior at different temperatures and the heteromeric coiled-coil complex is less thermostable than those obtained with the linear dimers.

2.3. Self-Assembly of K4 Dimers

The CD study revealed that the linear K4 dimers have increased helicities and T_ms in comparison to monomeric K4. Based on the structure of the linear K4 dimeric peptides, we hypothesize that either a hairpin structure or a 'tetramer-like' homodimer structure may form. If intra-homodimerization to form a hairpin occurs, the (dis)-assembly should be concentration-independent. However, if intermolecular dimerization occurs and "tetramer-like" homodimers are formed, the CD spectrum is expected to be concentration-dependent. Therefore, a concentration-dependent CD titration assay was performed (Figure S1d, Supporting Information).[16] A significant change in CD signal as a function of linear K4 dimer concentration was observed, suggesting that these linear K4 dimers form tetramer-like homodimeric structures instead of hairpin structures. The dimerization affinity constant, K_a was determined for NK4 and CK4 (Table S4, Supporting Information). CK4 has a higher K_a, which is consistent with the slightly increased stability of CK4 in comparison to NK4. A representation of the possible tetramer-like homodimers of NK4 and CK4 is described (Scheme S2a, Supporting Information). Homodimer formation may influence membrane fusion as homodimerization blocks the hydrophobic face of the helical peptide, hindering coiled-coil formation with E4.

PK4 consists of two K4 peptides connected by a disulfide bond between cysteines at *f* positions.[17] This arrangement means PK4 has two exposed hydrophobic faces, which makes the structure susceptible to higher order self-assembly. Indeed, PK4 shows a completely different CD spectrum compared to other peptides (Figure 1a). To study the self-assembly behavior of PK4 further, dynamic light scattering (DLS) studies were performed. PK4 showed very different hydrodynamic sizes and PDI in buffers (Table S5, Supporting Information). We then used the derived count rate (DCR) as an indicator of particle formation, as this reading is dependent on particle concentration and size. We compared the behavior of PK4 to the linear K4-dimers and peptide K4 in both H_2O and phosphate buffered saline (PBS). In H_2O, no particles formed as evidenced by the low DCR for all peptides (Figure S2a,

Supporting Information). In PBS, a high DCR was obtained for PK4, while the other peptides show a very low DCR, revealing the tendency of PK4 to aggregate. This finding is in line with the CD data of PK4, which can be explained by aggregation causing light scattering, which results in distortion of the spectrum. Thus, we conclude that PK4 self-assembles to form large aggregates as a result of shielding the exposed hydrophobic faces of the peptides from the solvent (Scheme S2b, Supporting Information). To verify this hypothesis, a DLS titration assay was performed, where peptide E4 was titrated into a solution of PK4 (Figure S2b, Supporting Information). Coiled-coil formation between peptide E/K is stronger than homodimerization,[14c] thus the addition of peptide E4 should result in the disappearance of large assemblies. At a low E/K ratio, the DCR gradually increased. This might be because E4 initially interacts with PK4 peptides at the edges of the assembled particles, resulting in the size increase. With additional amounts of E4, the DCR decreased dramatically. A low DCR was obtained when two equivalents of E4 were added, which indicates that large assemblies were no longer present. Thus, the DLS titration assay revealed that PK4 forms coiled-coils with peptide E4 at a 1:2 stoichiometric ratio.

The CD study reveals that the secondary structure of PK4 depends on temperature (Figure S1b, Supporting Information). Therefore, a temperature-dependent DLS assay was also performed (Scheme S2c, Supporting Information). The highest DCR was observed at 25 °C, suggesting the presence of large particles at this temperature (Figure S2c, Supporting Information). Increasing the temperature further resulted in a decrease of the DCR, revealing that the PK4 assemblies gradually dissociate, consistent with the temperature-dependent CD spectra of PK4. Upon heating, we assume the particles gradually dissociate to fully dissociated isolated dimers or small assemblies resulting in a CD spectrum typical for α-helices, and further heating resulted in the unfolding of the peptide. Surprisingly, no particles reformed upon slowly cooling from 90 to 20 °C as the DCR remained low. This suggests that upon cooling, the PK4 monomers form more thermodynamically stable, homomeric coiled-coil assemblies which further self-assemble into more homogeneous small particles (Scheme S2c, Supporting Information). To study whether the speed of cooling influences PK4 self-assembly, the experiment was repeated with fast cooling to 20 from 90 °C within 2 min. A high DCR close to the initial value was obtained, revealing that large particles were reformed after fast cooling. Moreover, PK4 displayed different hydrodynamic sizes under different cooling speeds (Table S5, Supporting Information). This shows that these large particles are kinetically-trapped assemblies while the smaller particles are in the more stable thermodynamically favored state.

2.4. Membrane Affinity of K4 Dimers

As described previously, peptide K4 plays an essential role in the E/K coiled-coil membrane fusion system because it induces membrane curvature, facilitating membrane fusion.[17] The lysine snorkeling mechanism was proposed to explain the interaction between the lysine-rich K peptides and the lipid membrane,[14b] which suggests that structural specificity plays a crucial role in peptide-membrane affinity. Peptide K4 adopts a helical structure in which the hydrophobic amino acids (at the "*a*" and "*d*" positions) form one face of the peptide while the lysines (at "*e*" and "*g*" positions) lie on both sides of this hydrophobic face. When interacting with a lipid membrane, the hydrophobic face of the peptide inserts into the hydrophobic center of the membrane, and the positive amines on the side chains of lysines interact with the negative phosphate groups of the lipid through electrostatic interactions. Therefore, the K4 dimers in the current study are expected to have a high affinity for lipid bilayers.

Tryptophan is intrinsically fluorescent and its fluorescence is sensitive to its environment; insertion into a hydrophobic membrane leads to a fluorescence increase. To compare the membrane partition coefficient (K_p) of the K4 peptide variants, a tryptophan fluorescence titration assay was performed (**Figure 2**a; and Table S6, Supporting Information). The tryptophan fluorescence of PK4 increased nearly fivefold in the presence of a lipid membrane. In contrast, the fluorescence of the linear K4 dimers hardly increased, revealing an inability to interact with a lipid membrane. The K_p of each peptide was determined by a nonlinear fitting procedure (Figure 2b). The highest partition coefficient was found using PK4, revealing that this dimer has the highest lipid membrane affinity. Although the linear K4 dimers are identical in composition, though different in structure to PK4, they show a low affinity for lipid membranes. This result can be explained by the fact that linear K4 dimers form "tetramer-like" dimeric structures which shield the hydrophobic faces of the peptides. As a result, these linear dimers have a low affinity for lipid membranes.

2.5. Simulation Analysis of K4 Dimers

Although shorter versions of E/K peptides have been examined using molecular dynamics (MD) simulations previously,[14b,18] longer peptides and in particular dimers thereof have not been studied before. Therefore, we performed an all-atom MD simulation to evaluate the most probable secondary structure of the PK4 dimer. The stable conformations of a K4 peptide and a PK4 dimer along a 300 ns simulation pathway are shown in Figure S3a,b (Supporting Information). The simulation reveals that the helical nature of the PK4 dimer is conserved for the entire simulated trajectory. While the considered timescale is rather short compared to the typical reorganization dynamics, it is sufficient to conclude that the helical nature of the dimer is better conserved than that of its monomeric counterpart. A longer 1000 ns simulation of a system containing an initially random dispersion of 6 PK4 dimers, see Figure S3c (Supporting Information) and Video S1 (Supporting Information), shows that dimers spontaneously aggregate into a higher order structure that lacks apparent order. Apart from the transient and very restricted uncoiling of individual PK4 dimers at their termini, the overall helical character of the PK4 dimers is well conserved.

Different roles of the K and E peptides were previously proposed.[14b] The membrane affinity of the K peptide and its projected only partial insertion into the membrane enables the formation of a coiled-coil with an E peptide. This idea agrees well with an inventory of amphipathic/amphiphilic peptides, in which peptide K resides in the A1 category that interacts with

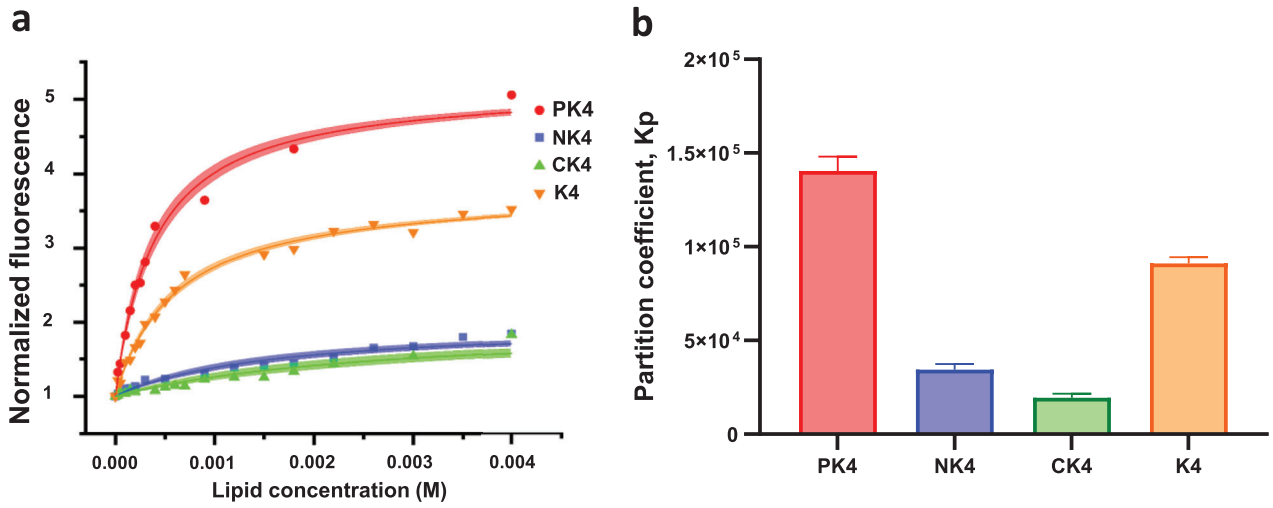

Figure 2. Membrane affinity evaluation. a) Tryptophan fluorescence titration assays to study the membrane affinity of each peptide: nonlinear fitting was based on equation 3 (see materials and methods). The shadow following each fitting curve represents the 95% confidence interval. b) The membrane partition coefficient (Kp) of three K4 dimers and K4 monomer was calculated during fitting.

zwitterionic lipid bilayers, while membrane binding of the E peptide is predicted to be unfavored.[19] For the dimeric K4 system, membrane affinity was also proven (Figure 2) and molecular details are provided by all-atom MD (AAMD) simulations for individual membrane-peptide setups. We find that the PK4 dimer has a higher membrane affinity than peptide K4, as demonstrated by the minimum distance histogram calculated for both 1,2-dioleoyl-sn-glycero-3-phosphocholine (DOPC) and 1,2-dioleoyl-sn-glycero-3-phosphoethanolamine (DOPE) membrane components (**Figure 3**a). In the presence of an E4 peptide (Figure 3b), the PK4 dimer interacts with the bilayer by inserting one hydrophobic side into the lipid bilayer, stabilizing the other side by complexation with the E4 peptide. This is fully in line with our hypothesis and suggests that the formation of such an E4/PK4 complex is preferred over E4 binding to the membrane, consistent with the experimental findings.

To simulate binding and restructuring processes at much larger time and length scales, we also performed coarse-grained (CG) MD. First, we considered the interaction of a single CPE4 (the E4 peptide conjugated to cholesterol via a poly(ethylene glycol) (PEG) spacer, for details, see the Supporting Information), which was introduced into the solution at a random position. Within the initial 50 ns, the lipopeptide gets bound to the membrane, with the cholesterol inserting itself spontaneously into the upper leaflet of the lipid membrane, in full agreement with experiments.[20] Interestingly, while the PEG linker remained in the water phase, the peptide remains close to the membrane. It should be noted that the subtle balance between membrane binding or solvation is sensitive to two factors in the CG model, particularly for the E4 peptide. Namely, the secondary peptide structure is necessarily fixed in the CG setup, preventing the peptide from uncoiling and adapting its solubility. Moreover, polarization may perturb the fine balance of the electrostatic interactions and screening. It has been shown that the structure of the ionic layer at the water/membrane interface is sensitive to such details. Given that this peptide is anchored to the membrane,[18c] however, we expect these factors to play only a rather insignificant role in our results.

After simulating the lipid membrane and CPE4 for 1 µs, two PK4 dimers were randomly placed in the solvent phase. While both K4 peptides of the PK4 dimers instantly move toward the lipid bilayer (see a snapshot, Figure 3c,d) in line with the affinity measurements (Figure 2), one K4 peptide binds irreversibly with the E4 peptide, and the other binds the lipid membrane and remains in this state during the entire simulation. We note that, in contrast to the AAMD results for a complex containing a PK4 dimer, the E4 peptide (red) positions itself slightly deeper into the membrane than the K4 peptide of PK4 (blue) that it binds (Figure 3e). The second, free, K4 peptide (light blue) of this dimer is also inserted slightly deeper than the E4-bound one (Figure 3e). Clearly, the preferred binding of E and K peptides is conserved at the CG level, but the position of the bound E4 peptide in the membrane differs. This can be explained by the factors mentioned before, but also by the membrane anchoring, due to its connectivity to the linker and membrane-embedded cholesterol group, which was not present in the AAMD setup. In particular, the binding characteristics of the second PK4 dimer, which does not form a complex with an E4 peptide, is found to agree very well with the AAMD case, i.e., only slightly varied in insertion depth and overall rather shallow (Figure 3a; and Figure S3a, Supporting Information). The radial distribution functions g(r) between the lipid PO4 group and all the peptides show that the membrane binding affinity is modulated by complex formation, see (Figure 3f). In particular, binding to the E4 peptide induces a small tilt to the dimer, making the unbound K4 peptide in the dimer complex more accessible from the solvent phase.

2.6. Liposome Fusion of K4 Dimers

The fusogenic properties of the different coiled-coil peptides were studied using lipid-mixing and content-mixing assays. Previous

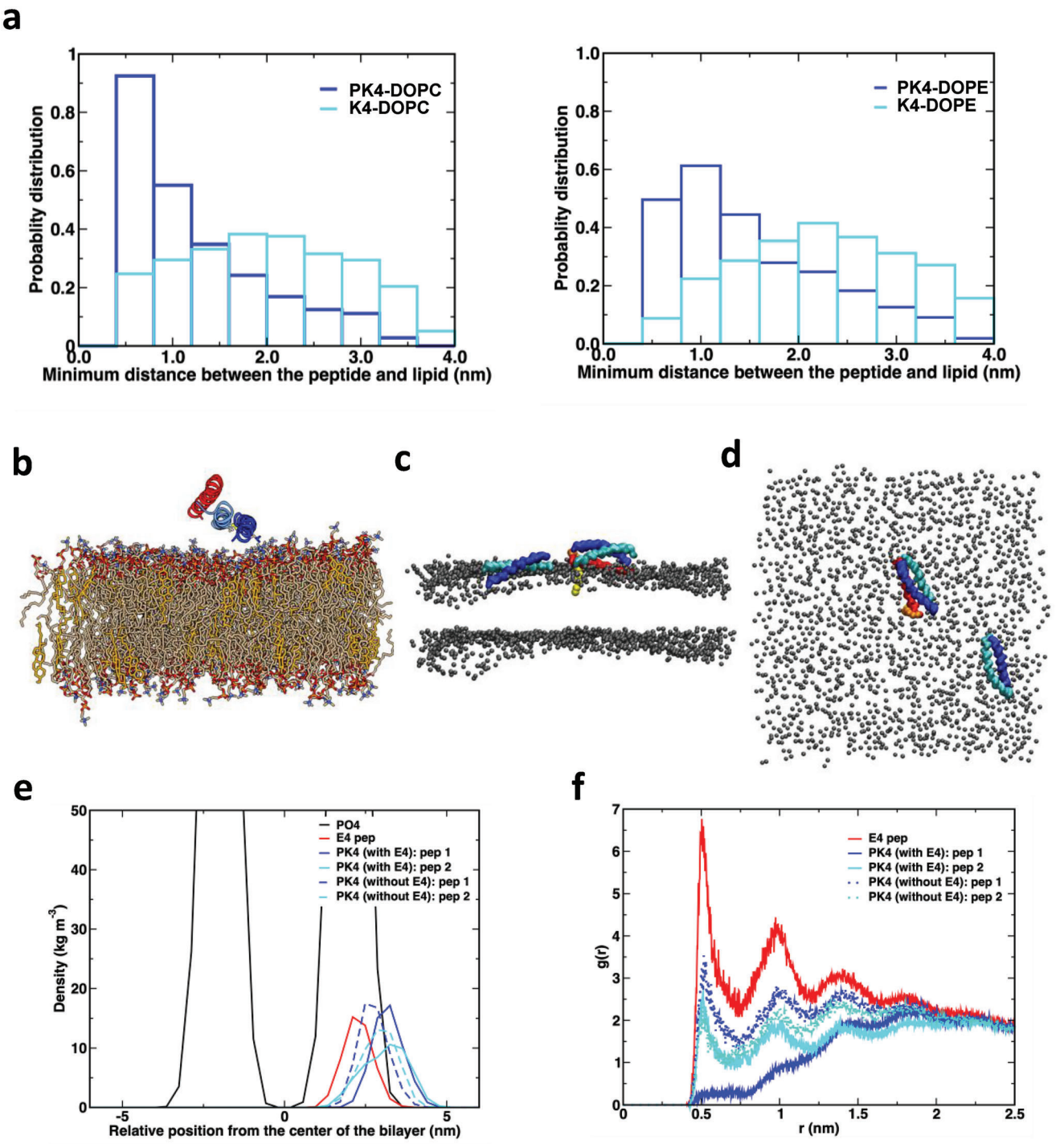

Figure 3. All-atom simulation results. a) Histogram of minimum distances between K4 peptide or PK4 dimer and DOPC (left) or DOPE (right) lipids, as obtained from the last 100 ns of the trajectory. b) Simulation snapshot of the lipid membrane with a single E4 (red) and a dimeric PK4 peptide (blue). Carbon, nitrogen, oxygen, and phosphate atoms are shown in brown, blue, red, and orange in the stick representation, while hydrogen atoms and water are omitted for clarity. c,d) CG simulation results: c) side view and d) front view of a snapshot, showing the final position and orientation of PK4 dimer (blue), E4 peptide (red), and PEG (orange) with cholesterol in yellow, with PO4 in gray. Only the peptide backbone is shown and all other CG particles are omitted for clarity. e) Partial density profiles for the E4 peptide (red), the two K4 peptides in the E4/PK4 dimer complex (solid lines), the two K4 peptides in the other PK4 dimer (dashed lines), and lipid CG bead PO4 (gray), obtained by averaging over a time interval. The colors match the ones used in the snapshots. f) Radial distribution functions (g(r)) of PO4 and all peptides for the snapshot. The solid dark blue g(r) for the K4 that is part of the complex shows that this K4 is least bound to the membrane.

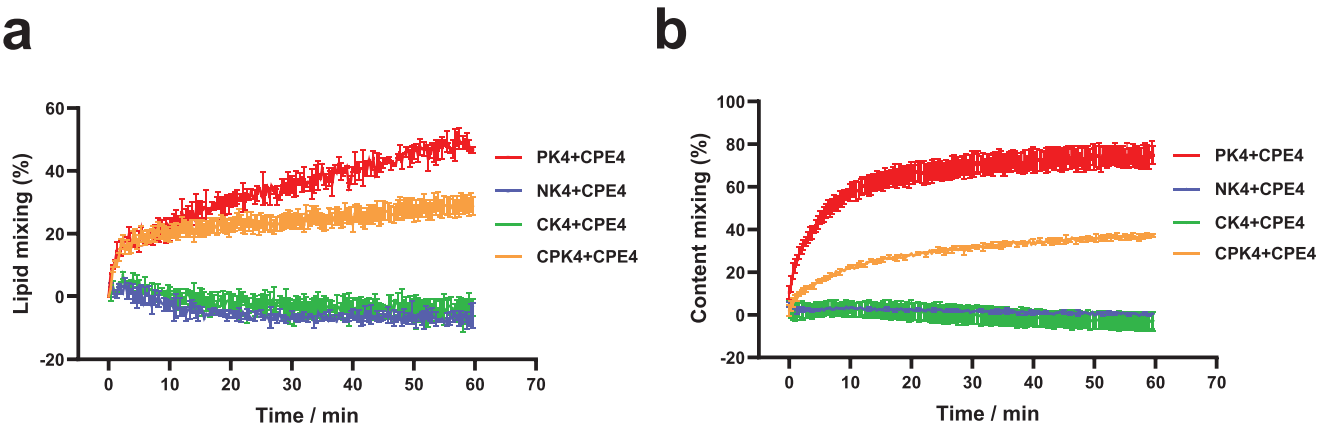

Figure 4. Liposome fusion of dimers. a) Lipid mixing of K4 dimers and K4 monomer with CPE4. b) Content mixing of K4 dimers and K4 monomer with CPE4. The number on the *y*-axis represents the percentage increase of fluorescence due to liposome hemifusion or membrane fusion.

studies have shown that the fusogenic properties are correlated to the stability of the peptides and the affinity of the K peptide to the lipid membrane.[18b,c] The combined physicochemical studies revealed that PK4 forms a strong coiled-coil complex with peptide E4 and also has a high affinity for lipid membranes, rendering this design highly fusogenic if our hypothesis is correct.

Therefore lipid and content mixing assays were performed to validate this hypothesis. The lipid mixing assay was performed with the Förster resonance energy transfer (FRET) pair nitrobenzoxadiazole (NBD, donor fluorophore) and lissamine rhodamine (LR, acceptor fluorophore).[15,20a] These dyes were attached to lipids and incorporated into the same lipid membrane. When membrane fusion occurs between fluorescent lipid-modified liposomes and nonfluorescent liposomes, the average distance between the NBD and LR fluorophores increases, resulting in enhanced NBD emission. In this assay, both sets of liposomes contained 1% CPE4 and liposome fusion was initiated by K4 dimer addition. For comparison, lipid mixing facilitated by CPK4, (the K4 peptide attached to a cholesterol lipid via a PEG spacer, for details, see the Supporting Information), and CPE4 was studied as well. PK4 addition triggered efficient lipid mixing in contrast to the two linear K4 dimers (**Figure 4**a). The lipid mixing efficiency of PK4/CPE4 is higher than that for CPK4/CPE4. In control experiments (Figure S4a, Supporting Information), a low fluorescence increase was observed when PK4 was added to plain liposomes (i.e., liposomes without CPE4), indicating a low level of nonspecific membrane fusion. In contrast to PK4, the linear K4 dimers cannot trigger fusion between CPE4 modified liposomes, probably due to their low lipid membrane affinity.

Next, a content mixing assay was performed. Liposomes were either loaded with sulphorhodamine-B (SRb) at a self-quenching concentration (20 mM) or contained only a buffer. Both liposomes were modified with 1% CPE4. Upon membrane fusion, content mixing results in SRb dilution and fluorescence dequenching. Efficient content mixing was obtained using PK4, while no fluorescence increase was observed for NK4 and CK4 (Figure 4b). As with lipid mixing, content mixing was significantly higher for PK4/CPE4 compared to CPK4/CPE4. As a control experiment (Figure S4b, supporting information), a leakage test was performed by mixing SRb liposomes with the different K4 dimers. PK4 induced some liposome leakage, but at a low level compared to the PK4/CPE4 induced content mixing. This finding is not surprising because PK4 has a very high affinity for lipid membranes. When PK4 was added to a liposome mixture containing non-CPE4 modified liposomes, the content mixing curve was slightly higher than the leakage control, revealing that even in the absence of CPE4, PK4 weakly induces liposome fusion, along with leakage. In contrast, no linear K4 dimer was able to induce non-CPE4 modified liposome fusion or leakage.

2.7. Cell Membrane Labeling Efficiency between Dimers

To confirm whether coiled-coil formation between K4-dimers and E4 also occurs at the cell membrane, a labeling assay was performed. HeLa cells were preincubated with CPE4 as described previously.[13c,20a] Next, the cells were treated with the various K4-dimers before Fluo-E4 was added (**Figure 5**a). Interestingly, cell membrane labeling efficiency varied between the various K4-dimers (Figure 5b). PK4 displayed the highest fluorescence on the cell membrane, indicating efficient coiled-coil formation between PK4 and CPE4. In contrast, the linear K4-dimers NK4 and CK4 showed a lower degree of fluorescence. We also studied the importance of pretreating cells with CPE4. Cells lacking CPE4 were incubated with PK4 and these also exhibited fluorescent cell membranes, albeit the observed fluorescence was not homogeneously distributed (Figure S5a, Supporting Information). Most likely, the positively charged PK4 peptides form aggregates, as shown by DLS (Figure S5b, Supporting Information), which bind to the negatively charged cell membrane via attractive electrostatic interactions. The addition of the linear dimers NK4 or CK4 to plain cells did not result in any detectable binding.

The differences in binding of the various K4-dimers were quantified by flow cytometry (Figure 5c). CPE4 pretreated cells revealed a high binding affinity for K4 and K4-dimers. In contrast, in the absence of CPE4 significantly lower peptide K(-dimer) binding was observed. These results were consistent with the CD and confocal imaging results. PK4-dimer associated effectively with the cell membrane by either forming coiled-coils with CPE4 or directly interacting with the cell membrane. In contrast, the linear dimers NK4 and CK4 showed a weaker ability to induce coiled-coil interactions, resulting in a low cell membrane affinity.

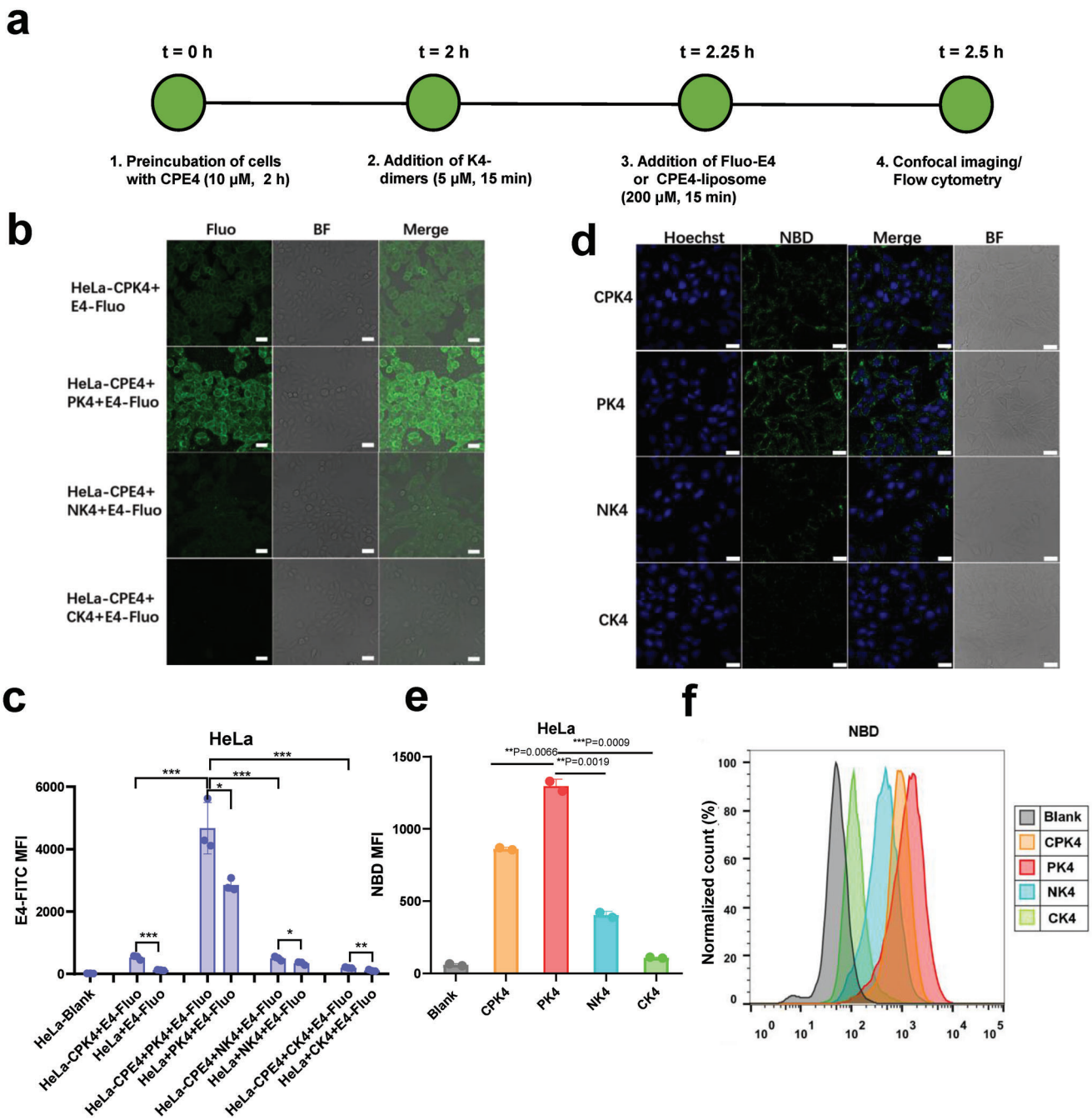

Figure 5. Cell labeling and cell uptake studies. a) Schematic representation of the cell labeling and cell uptake experiments of K4 dimer with cells. b) Confocal images of cell membrane labeling between K4 monomer/dimers and Fluo-E4. Green: fluorescein-E4; BF: bright field; scale bar is 30 μm. c) Quantification of cell membrane labeling efficiency by flow cytometry measurements. d) Confocal images of K4 monomer and dimers with fluorescent NBD-PE labeled CPE4-liposomes. e,f) Quantification of the liposome-NBD intensity of K4 monomer and dimers with cells. Green: PE-NBD; blue: Hoechst 33 342. BF: bright field; scale bar is 30 μm. In (d–f), CPK4: CPK4-cell+CPE4-liposome-NBD; PK4: CPE4-cell+PK4+CPE4-liposome-NBD; NK4: CPE4-cell+NK4+CPE4-liposome-NBD; CK4: CPE4-cell+CK4+CPE4-liposome-NBD. Unpaired student *t*-test was used to determine the significance of data comparisons (****$P < 0.0001$; ***$P < 0.001$; **$P < 0.01$; *$P < 0.05$). In all panels, error bars represent mean ± s.d. ($n = 3$).

2.8. Cell Uptake Efficiency of Dimers

After examining coiled-coil formation at the cell membrane between the K4-dimers and CPE4, cell uptake of CPE4-liposomes was investigated using the same approach. Again, cells were preincubated sequentially with CPE4 and the K4-dimers before fluorescent CPE4-liposomes were added and cell uptake was quantified (Figure 5a). As expected, CPE4-liposomes were homogeneously distributed on the cell membrane (Figure 5d). However, marked differences were observed for the different

K4-dimers. PK4 induced strong cell-liposome uptake efficiency, while the linear dimers NK4, and CK4 were less efficient. When the CPE4 preincubation step of cells was omitted, PK4 also induced some binding, but the fluorescence was randomly dispersed on the cell membrane (Figure S5c, Supporting Information). As mentioned earlier, attractive interactions between PK4 and the cell membrane might be the cause for this observation. As expected, the linear dimers NK4 and CK4 were unable to bind to cells without CPE4 preincubation. The cell uptake efficiency differences between groups were again quantified with flow cytometry (Figure 5e,f). Consistent with the confocal imaging, the PK4 coiled-coil dimer showed the highest cell uptake efficiency, which was superior to monomeric K4 and the linear dimers NK4 and CK4. Not surprisingly, in cells without CPE4 preincubation, the dimers resulted in weaker cell uptake efficiency (Figure S5d, Supporting Information). Combined, these studies revealed that PK4 interacts very efficiently with CPE4-preincubated cells.

2.9. Liposome-Cell Membrane Fusion—NBD/Propidium Iodide (PI) Delivery by Dimers

Next, membrane fusion between liposomes and cells was studied using propidium iodide (PI) as a model drug. This dye binds to DNA and is membrane impermeable requiring a carrier to enter cells.[19,21] Cells were sequentially pretreated with CPE4 and the K4-dimers before PI encapsulated in CPE4-liposomes was added to induce liposome-cell membrane fusion and concomitant PI delivery (**Figure 6**a). Confocal imaging showed the green fluorescent dye NBD incorporated into CPE4-liposomes, evenly distributed on cell membranes, while PI was observed in the cytosol and nucleus of cells (Figure 6b). As expected, CPE4-liposomes were able to deliver PI into cells pretreated with CPK4, consistent with our previous study.[13c] Importantly, PK4 induced the highest PI delivery inside cells and the dye was present in the cytosol and nucleus. In contrast, the linear K4-dimers induced a low PI delivery efficiency. NK4 induced weak fluorescence both on the cell membrane and in the cytoplasm, and almost no membrane and cytoplasm fluorescence was observed when CK4 was used. When the cells were not pretreated with CPE4, PK4 was still able to induce liposome-cell fusion resulting in some PI uptake (Figure S6a, Supporting Information). Furthermore, liposomes lacking CPE4 showed neither PI delivery nor NBD-labeling of the cell plasma membrane irrespective of the K-dimer used (Figure S6b, Supporting Information). Next, the same experiment was performed using Chinese hamster ovary (CHO) cells to confirm that PI delivery is cell-type independent. Consistent with the results in HeLa cells, PI was observed in CHO cells when PK4 was used, while CPK and the linear K-dimers were less efficient (Figure S7a, Supporting Information). Again, omitting the CPE4 preincubation step resulted in inefficient PI delivery (Figure S7b, Supporting Information).

In summary, these results revealed that all K4-dimers mediate cell-liposome membrane fusion resulting in cytosolic and nuclear PI delivery. The PK4-dimer outperformed all other designs due to the enhanced coiled-coil interaction between PK4 and E4, combined with the membrane affinity of PK4 facilitating efficient PI delivery efficiency.

2.10. Delivery of Doxorubicin

After demonstrating that K4-dimers efficiently mediated liposomal PI delivery into cells via membrane fusion, drug delivery efficiency, and subsequent pharmacological effects were further evaluated using doxorubicin (DOX) (Figure 6a). This drug is an effective and frequently used chemotherapeutic agent for various malignancies, but cardiomyopathy is a life-threatening side effect.[22] Therefore targeted DOX delivery is highly desirable because it would increase the therapeutic dose while limiting the side effects. Furthermore, DOX becomes more fluorescent upon binding to DNA and tRNA, making it suitable for cellular imaging and quantification.

CPE4-preincubated cells were treated with the K4-dimers before CPE4-liposomes containing DOX were added. Confocal imaging confirmed successful DOX delivery as its fluorescence was observed in both the nucleus and cytosol of cells (Figure 6c). Again, PK4 induced the most effective DOX cellular delivery, as compared to the linear K4-dimers or CPK4. Untreated cells showed negligible DOX delivery confirming that CPE4 and K4-dimers are required for efficient drug delivery (Figure S8a, Supporting Information).

DOX delivery was quantified by flow cytometry. All coiled-coil pairs facilitated liposome-cell fusion resulting in a high percentage of DOX positive cells: >85% in all cases (Figure 6d), indicative of efficient DOX delivery. Importantly, the internalized DOX intensities varied significantly between the groups. In line with all previous results, PK4 achieved the highest DOX intensities in cells as compared to CPK4 and the linear K4-dimers (Figure 6e,f). DOX was delivered by PK4 to cells that were not pretreated with CPE4, albeit with a lower intensity than CPE4-preincubated cells. All control groups did not show significant DOX delivery (Figure S8b, Supporting Information). These results demonstrate that the CPE4/PK4 pair achieved the highest DOX delivery in all experimental groups.

2.11. DOX Uptake Efficiency after Application of Endocytosis Inhibitors

CPE4/CPK4-mediated fusion of liposomes with cells was confirmed in a previous study using well-known endocytosis inhibitors.[13c] In this study, PK4 was the most efficient at delivering content to cells and therefore we studied its uptake mechanism in the presence of common endocytosis inhibitors. After incubation of cells with the endocytosis inhibitors, the uptake of liposomes and concomitant delivery of content were quantified. Flow cytometry was employed to quantify the intensity differences of internalized DOX with each endocytosis inhibitor treatment and compared to delivery in the absence of the inhibitors. Since the PK4-dimer is positively charged, we included cationic non-fusogenic liposomes (DOTAP: DOPC, 1:1) in this study for comparison.

The cellular uptake of cationic liposomes was greatly inhibited in the presence of NaN_3, MβCD, wortmannin, and incubation at 4 °C. This experiment revealed that cationic liposome uptake is energy-dependent, mainly driven by micropinocytosis, and depends on lipid raft integrity (Figure S9a, Supporting Information).[23]

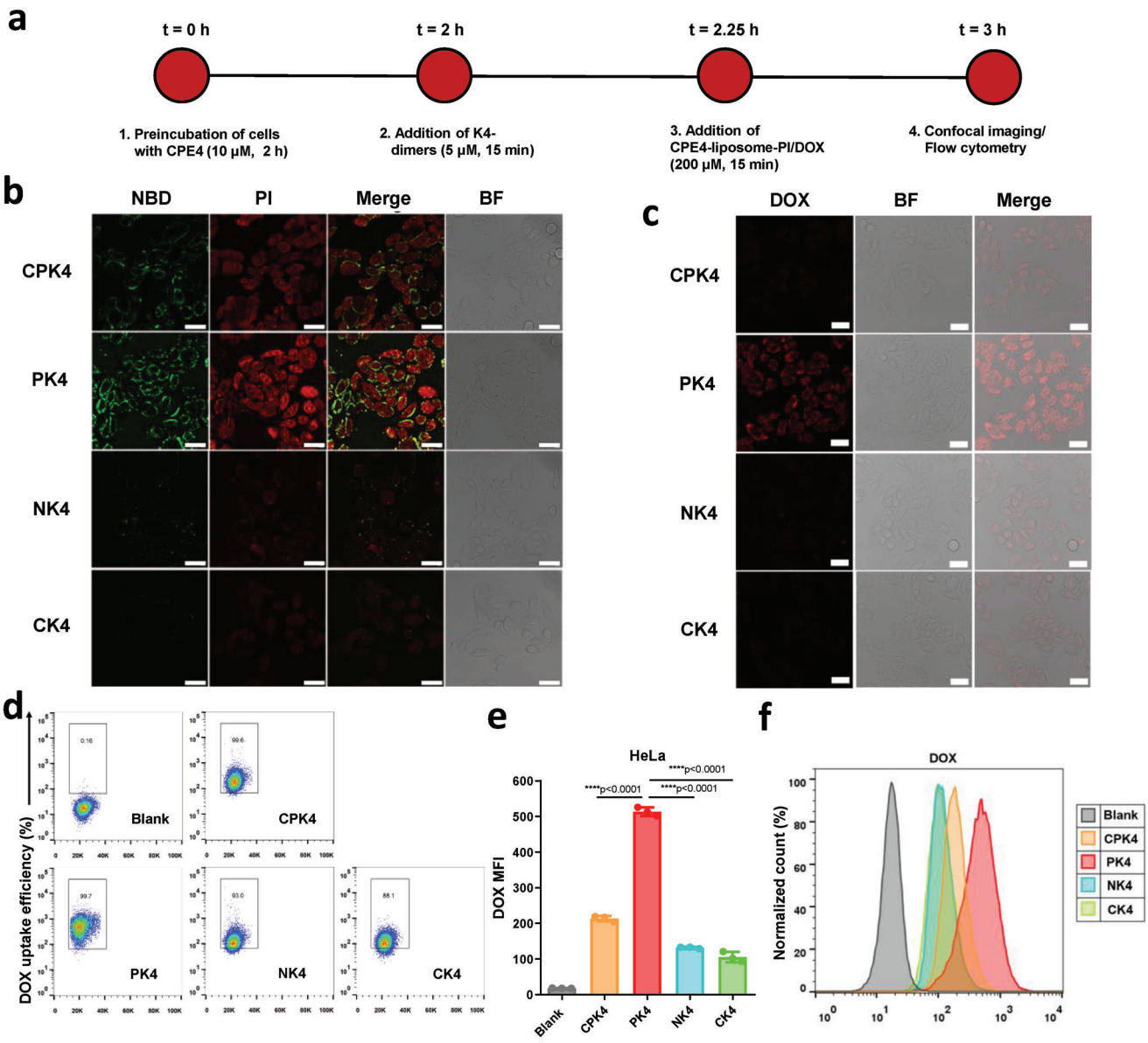

Figure 6. Liposomal delivery (PI and DOX) to cells. a) Schematic representation of the liposomal delivery of PI and DOX to cells. b) Confocal images of liposomal PI delivery by K4 monomer and dimers. Green: NBD-PE; red: PI; BF: bright field; scale bar is 30 μm. CPK4: CPK4-cell+CPE4-liposome-NBD-PI; PK4: CPE4-cell+PK4+CPE4-liposome-NBD-PI; NK4: CPE4-cell+NK4+CPE4-liposome-NBD-PI; CK4: CPE4-cell+CK4+CPE4-liposome-NBD-PI. c) Confocal images of DOX uptake facilitated by K4 monomer and dimers in HeLa cells. Red: DOX; BF: bright field; scale bar is 30 μm. d) Quantification of DOX uptake percentages facilitated by K4 monomer and dimers in HeLa cells. e,f) Quantification of internalized DOX intensity facilitated by K4 monomer and dimers. In c-f, CPK4: CPK4-cell+CPE4-liposome-DOX; PK4: CPE4-cell+PK4+CPE4-liposome-DOX; NK4: CPE4-cell+NK4+CPE4-liposome-DOX; CK4: CPE4-cell+CK4+CPE4-liposome-DOX. Unpaired student *t*-test was used to determine the significance of data comparisons (****$P < 0.0001$; ***$P < 0.001$; **$P < 0.01$; *$P < 0.05$). In all panels, error bars represent mean ± s.d. ($n = 3$).

Next, the effect of endocytosis inhibitors on cellular uptake of liposomes encapsulating DOX using the PK4 coiled-coil dimer was investigated (**Figure 7**a). Most of the endocytosis inhibitors seemed to have a minimal effect on DOX uptake efficiency except for MβCD, which disrupts the cholesterol-rich caveolae-containing membrane microdomains by removing cholesterol from the plasma membrane.[23b–d] Unlike the cationic DOTAP liposomes, the ATP energy depleting agent NaN_3 exerted no effect on the uptake efficiency for PK4-dimer,[23a] only incubation at 4 °C reduced the uptake efficiency slightly. These findings demonstrated that the cellular uptake of the PK4-dimer was mainly driven by membrane fusion independent of energy consumption, and also demands lipid integrity. We also tested the endocytosis inhibitors' effect on the PK4-dimer when the cells were not pretreated with CPE4 (Figure S9b, Supporting Information). Similar to the PK4 coiled-coil pair, MβCD, and 4 °C incubation resulted in a reduction in cellular uptake to <20%. Meanwhile, nocodazole and dynasore reduced the cellular uptake

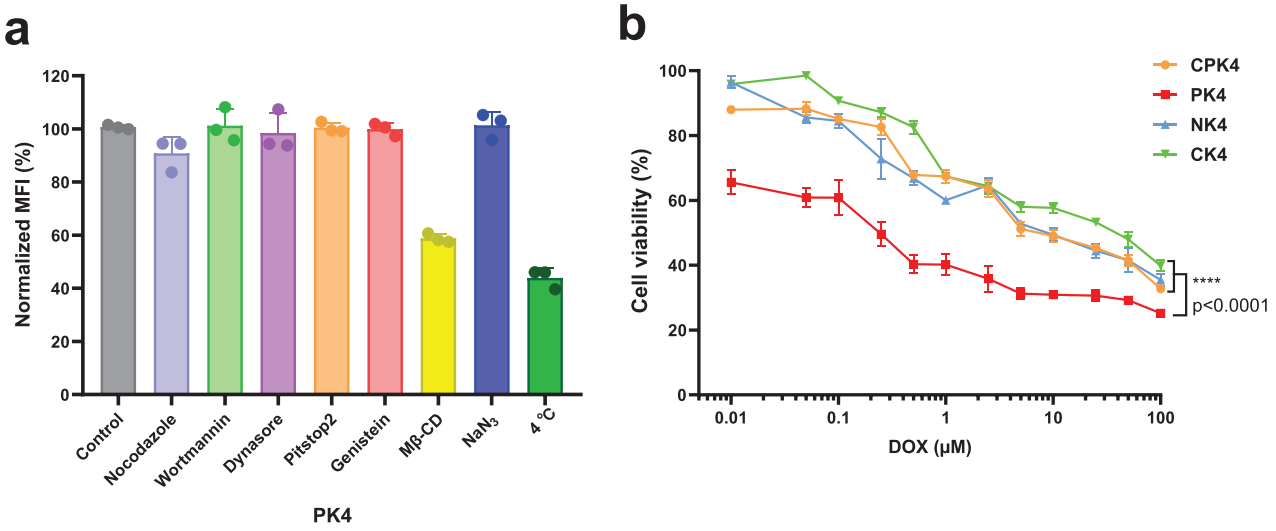

Figure 7. Uptake mechanism and antitumor effect. a) Quantification of DOX uptake in HeLa cells in the presence of endocytosis inhibitors. b) Cytotoxicity evaluation of K4 monomer and dimers after delivery of DOX. CPK4: CPK4-cell+CPE4-liposome-DOX; PK4: CPE4-cell+PK4+CPE4-liposome-DOX; NK4: CPE4-cell+NK4+CPE4-liposome-DOX; CK4: CPE4-cell+CK4+CPE4-liposome-DOX. Two-way ANOVA analysis was used to determine the significance of data comparisons (****$P < 0.0001$; ***$P < 0.001$; **$P < 0.01$; *$P < 0.05$). In all panels, error bars represent mean ± s.d. ($n = 3$).

by about 25% and 15%, respectively, indicating micropinocytosis and clathrin-mediated endocytosis were also involved.[24] Taken together, these results prove that cellular DOX uptake of the PK4-dimer was mainly induced by membrane fusion requiring the presence of cholesterol. Due to the positive charges of the PK4 particles, it could also partially facilitate the lipopeptide CPE4-modified liposomes entering the cell through endocytosis, and this could further facilitate cellular delivery.

2.12. In Vitro Antitumor Effect Evaluation after Delivery of DOX

After confirming that CPE4/PK4 delivers liposomal DOX efficiently into cells, the antitumor effect induced by DOX delivery was evaluated. HeLa cells were decorated with CPE4, treated with the K4-dimers, and then incubated for 2 h with CPE4-modified liposomes encapsulating DOX. Next, the cell viability was determined after 36 h. Efficient DOX cellular uptake requires both peptides to be present, thus we mainly focused on the comparison of the HeLa cytotoxicity differences between K4 monomer and dimers in which both peptides were included after the delivery of DOX. The K4 monomer and dimers induced an in vitro antitumor effect in a concentration-dependent manner (Figure 7b). The parallel PK4-dimer induced potent cytotoxicity, and the viability of HeLa cells was significantly lower than with the monomer and linear dimers for all the concentrations, demonstrating an improved antitumor effect by PK4-mediated delivery of DOX.

An MTT assay was used to demonstrate that the peptides and liposomes in the absence of DOX were nontoxic. For this, cells were decorated with CPE4, and the K4-dimers were added, followed by the addition of CPE4-modified liposomes (without encapsulated DOX). The cell viability remained high (> 90%) irrespective of liposome concentrations, demonstrating that the peptides are not toxic (Figure S9c, Supporting Information). Taken together, we showed that coiled-coil peptide dimers can be safely applied to facilitate cellular drug delivery, and the CPE4/PK4 pair can induce highly efficient cellular liposomal delivery with an enhanced therapeutic effect after loading antitumor drugs into the liposomes.

3. Conclusion

We designed three coiled-coil peptide-K dimers, PK4, NK4, and CK4, by varying the conjugation position and investigated their structural differences, cellular uptake efficiency, and pharmacological effects after encapsulating an antitumor drug. CD spectroscopy revealed distinct differences in helical structure between dimers, and PK4 exhibited the strongest coiled-coil interactions with the complementary peptide E4. The cell membrane labeling assay showed that PK4 triggered the highest cell membrane affinity while linear K4-dimers hardly interacted with the cell membrane. Cellular uptake studies showed liposome delivery into cells was dependent on the dimer used. Among the three dimers, PK4 elicited the strongest cellular liposomal delivery and DOX cellular uptake. The uptake mechanism study proved that efficient liposomal DOX delivery achieved using PK4 was mainly mediated by membrane fusion, although endocytosis was partially involved due to the nonspecific interactions between positively charged PK4 and cell membranes. Consistent with the DOX cellular uptake result, a cytotoxicity evaluation confirmed PK4 induced an enhanced antitumor effect in vitro, which was superior to CPK4 and the linear dimers NK4 and CK4. Computational evaluation using all-atom and coarse-grained molecular dynamics provided detailed insights into the binding properties of the peptides at the molecular level, further corroborating their anticipated role in fusion. These results indicate that PK4 possesses the strongest coiled-coil interaction with peptide E,

leading to significant membrane fusion and concomitant efficient cellular liposomal delivery. Moreover, the high affinity of PK4 to lipid membranes aids fusion. In comparison, coiled-coil formation of linear dimers is notably weak and their lipid membrane affinity is also low, therefore they are unable to induce efficient membrane fusion. These results confirm our hypothesis that the dimerization of peptide K could increase membrane fusion and lipid affinity, which is pivotal for achieving enhanced liposomal drug delivery. In summary, this study of peptide dimerization design and their cellular delivery evaluation not only contributes to the design and development of coiled-coil peptide-based membrane fusion systems but also provides a more efficient system for future drug delivery applications.

Supporting Information

Supporting Information is available from the Wiley Online Library or from the author.

Acknowledgements

The authors acknowledged the financial support of the Dutch Research Council (NWO) to A.K. via a VICI Grant (724.014.001) and the Chinese Scholarship Council for a CSC grant to Y.Z. and M.S. [Correction added after publication 13 September 2023: Aimee L. Boyle was added as additional corresponding author.]

Conflict of Interest

The authors declare no conflict of interest.

Data Availability Statement

The data that support the findings of this study are available from the corresponding author upon reasonable request.

Keywords

cell-liposome membrane fusion, coiled-coil peptide, drug delivery, membranes, peptide–membrane interactions

Received: February 8, 2023
Revised: April 6, 2023
Published online: May 18, 2023

[1] a) O. C. Farokhzad, R. Langer, *Adv. Drug Delivery Rev.* **2006**, *58*, 1456; b) R. K. Jain, T. Stylianopoulos, *Nat. Rev. Clin. Oncol.* **2010**, *7*, 653; c) D. A. Scheinberg, C. H. Villa, F. E. Escorcia, M. R. McDevitt, *Nat. Rev. Clin. Oncol.* **2010**, *7*, 266.

[2] a) J. Shi, P. W. Kantoff, R. Wooster, O. C. Farokhzad, *Nat. Rev. Cancer* **2017**, *17*, 20; b) C. Zhang, L. Yan, X. Wang, S. Zhu, C. Chen, Z. Gu, Y. Zhao, *Nano Today* **2020**, *35*, 101008; c) J. Wolfram, M. Ferrari, *Nano Today* **2019**, *25*, 85.

[3] a) I. Canton, G. Battaglia, *Chem. Soc. Rev.* **2012**, *41*, 2718; b) G. Sahay, D. Y. Alakhova, A. V. Kabanov, *J. Control. Release* **2010**, *145*, 182.

[4] a) E. Ruoslahti, *Adv. Drug Delivery Rev.* **2017**, *110*, 3; b) C. Zhang, W. Wu, R.-Q. Li, W.-X. Qiu, Z.-N. Zhuang, S.-X. Cheng, X.-Z. Zhang, *Adv. Funct. Mater.* **2018**, *28*, 1804492.

[5] a) S. Jang, S. Hyun, S. Kim, S. Lee, I. S. Lee, M. Baba, Y. Lee, J. Yu, *Angew. Chem.* **2014**, *126*, 10250; b) D. M. Copolovici, K. Langel, E. Eriste, Ü. Langel, *ACS Nano* **2014**, *8*, 1972.

[6] a) B. R. Meade, S. F. Dowdy, *Adv. Drug Delivery Rev.* **2007**, *59*, 134; b) H. Cheng, J.-Y. Zhu, X.-D. Xu, W.-X. Qiu, Q. Lei, K. Han, Y.-J. Cheng, X.-Z. Zhang, *ACS Appl. Mater. Interfaces* **2015**, *7*, 16061.

[7] a) W. B. Kauffman, T. Fuselier, J. He, W. C. Wimley, *Trends Biochem. Sci.* **2015**, *40*, 749; b) J. P. Richard, K. Melikov, E. Vives, C. Ramos, B. Verbeure, M. J. Gait, L. V. Chernomordik, B. Lebleu, *J. Biol. Chem.* **2003**, *278*, 585; c) A. F. L. Schneider, M. Kithil, M. C. Cardoso, M. Lehmann, C. P. R. Hackenberger, *Nat. Chem.* **2021**, *13*, 530.

[8] a) S. H. Nam, J. Jang, D. H. Cheon, S.-E. Chong, J. H. Ahn, S. Hyun, J. Yu, Y. Lee, *J. Control. Release* **2021**, *330*, 898; b) X. Guo, L. Wang, K. Duval, J. Fan, S. Zhou, Z. Chen, *Adv. Mater.* **2018**, *30*, 1705436.

[9] a) S. Pescina, C. Ostacolo, I. M. Gomez-Monterrey, M. Sala, A. Bertamino, F. Sonvico, C. Padula, P. Santi, A. Bianchera, S. Nicoli, *J. Control. Release* **2018**, *284*, 84; b) G. Guidotti, L. Brambilla, D. Rossi, *Trends Pharmacol. Sci.* **2017**, *38*, 406; c) N. Vale, D. Duarte, S. Silva, A. S. Correia, B. Costa, M. J. Gouveia, A. Ferreira, *Pharmacol Res* **2020**, *162*, 105231; d) K. Desale, K. Kuche, S. Jain, *Biomater. Sci.* **2021**, *9*, 1153.

[10] a) F. Zhang, A. Angelova, V. M. Garamus, B. Angelov, S. Tu, L. Kong, X. Zhang, N. Li, A. Zou, *ACS Appl. Mater. Interfaces* **2021**, *13*, 35281; b) Z. Kang, G. Ding, Z. Meng, Q. Meng, *Peptides* **2019**, *121*, 170149.

[11] a) C. Südhof Thomas, E. Rothman James, *Science* **2009**, *323*, 474; b) R. Jahn, R. H. Scheller, *Nat. Rev. Mol. Cell Biol.* **2006**, *7*, 631; c) Y. A. Chen, R. H. Scheller, *Nat. Rev. Mol. Cell Biol.* **2001**, *2*, 98.

[12] H. R. Marsden, I. Tomatsu, A. Kros, *Chem. Soc. Rev.* **2011**, *40*, 1572.

[13] a) L. Kong, S. H. C. Askes, S. Bonnet, A. Kros, F. Campbell, *Angew. Chem., Int. Ed.* **2016**, *55*, 1396; b) J. Yang, Y. Shimada, R. C. L. Olsthoorn, B. E. Snaar-Jagalska, H. P. Spaink, A. Kros, *ACS Nano* **2016**, *10*, 7428; c) J. Yang, A. Bahreman, G. Daudey, J. Bussmann, R. C. L. Olsthoorn, A. Kros, *ACS Cent. Sci.* **2016**, *2*, 621.

[14] a) G. A. Daudey, M. Shen, A. Singhal, P. van der Est, G. J. A. Sevink, A. L. Boyle, A. Kros, *Chem. Sci.* **2021**, *12*, 13782; b) M. Rabe, C. Aisenbrey, K. Pluhackova, V. de Wert, Aimee L. Boyle, Didjay F. Bruggeman, Sonja A. Kirsch, Rainer A. Böckmann, A. Kros, J. Raap, B. Bechinger, *Biophys. J.* **2016**, *111*, 2162; c) M. Rabe, H. R. Zope, A. Kros, *Langmuir* **2015**, *31*, 9953; d) M. Rabe, C. Schwieger, H. R. Zope, F. Versluis, A. Kros, *Langmuir* **2014**, *30*, 7724; e) K. Pluhackova, T. A. Wassenaar, S. Kirsch, R. A. Böckmann, *J. Phys. Chem. B* **2015**, *119*, 4396.

[15] H. Robson Marsden, N. A. Elbers, P. H. H. Bomans, N. A. J. M. Sommerdijk, A. Kros, *Angew. Chem., Int. Ed.* **2009**, *48*, 2330.

[16] N. S. A. Crone, A. Kros, A. L. Boyle, *Bioconjugate Chem.* **2020**, *31*, 834.

[17] J. M. Mason, K. M. Arndt, *ChemBioChem* **2004**, *5*, 170.

[18] a) D. A. Lindhout, J. R. Litowski, P. Mercier, R. S. Hodges, B. D. Sykes, *Biopolymers* **2004**, *75*, 367; b) G. Pähler, C. Panse, U. Diederichsen, A. Janshoff, *Biophys. J.* **2012**, *103*, 2295; c) M. Bulacu, G. J. A. Sevink, *Biochim. Biophys. Acta, Biomembr.* **2015**, *1848*, 848.

[19] D. Agudelo, P. Bourassa, G. Bérubé, H. A. Tajmir-Riahi, *J. Photochem. Photobiol., B* **2016**, *158*, 274.

[20] a) H. R. Zope, F. Versluis, A. Ordas, J. Voskuhl, H. P. Spaink, A. Kros, *Angew. Chem., Int. Ed.* **2013**, *52*, 14247; b) F. Versluis, J. Voskuhl, B. van Kolck, H. Zope, M. Bremmer, T. Albregtse, A. Kros, *J. Am. Chem. Soc.* **2013**, *135*, 8057.

[21] a) C. Pérez-Arnaiz, N. Busto, J. M. Leal, B. García, *J. Phys. Chem. B* **2014**, *118*, 1288; b) F. Zunino, A. Di Marco, A. Zaccara, R. A. Gambetta, *Biochim. Biophys. Acta* **1980**, *607*, 206.

[22] a) K. Chatterjee, J. Zhang, N. Honbo, J. S. Karliner, *Cardiology* **2010**, *115*, 155; b) G. Takemura, H. Fujiwara, *Prog. Cardiovasc. Dis.* **2007**, *49*, 330.

[23] a) S. Novakowski, K. Jiang, G. Prakash, C. Kastrup, *Sci. Rep.* **2019**, *9*, 552; b) D. Vercauteren, R. E. Vandenbroucke, A. T. Jones, J. Rejman, J. Demeester, S. C. De Smedt, N. N. Sanders, K. Braeckmans, *Mol. Ther.* **2010**, *18*, 561; c) S. K. Rodal, G. Skretting, Ø. Garred, F. Vilhardt,

B. van Deurs, K. Sandvig, *Mol. Biol. Cell* **1999**, *10*, 961; d) M. Marsh, A. Helenius, *Cell* **2006**, *124*, 729; e) C. Yao, P. Wang, X. Li, X. Hu, J. Hou, L. Wang, F. Zhang, *Adv. Mater.* **2016**, *28*, 9341; f) W. Tao, X. Mao, J. P. Davide, B. Ng, M. Cai, P. A. Burke, A. B. Sachs, L. Sepp-Lorenzino, *Mol. Ther.* **2011**, *19*, 567; g) A. Arcaro, M. P. Wymann, *Biochem. J.* **1993**, *296*, 297.

[24] a) D. Vercauteren, M. Piest, L. J. van der Aa, M. Al Soraj, A. T. Jones, J. F. J. Engbersen, S. C. De Smedt, K. Braeckmans, *Biomaterials* **2011**, *32*, 3072; b) E. Macia, M. Ehrlich, R. Massol, E. Boucrot, C. Brunner, T. Kirchhausen, *Dev. Cell* **2006**, *10*, 839; c) G. J. Doherty, H. T. McMahon, *Annu. Rev. Biochem.* **2009**, *78*, 857; d) G. Preta, J. G. Cronin, I. M. Sheldon, *Cell Commun. Signaling* **2015**, *13*, 24.